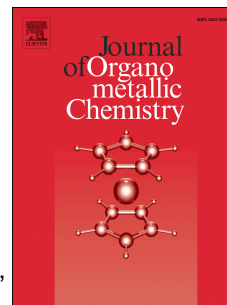


Accepted Manuscript

Diruthenium tetracarbonyl sawhorse complexes bearing N-heterocyclic carbene and phosphine ligands: Synthesis, structural characterization, and catalytic activity

Thomas N. Rorhabaugh, Jr., Joshua C. Doverspike, Steven J. Geib, Evan D. Sawyer, Mitchell R. Stibbard, Thomas J. Malosh



PII: S0022-328X(15)30205-9

DOI: [10.1016/j.jorganchem.2015.11.006](https://doi.org/10.1016/j.jorganchem.2015.11.006)

Reference: JOM 19293

To appear in: *Journal of Organometallic Chemistry*

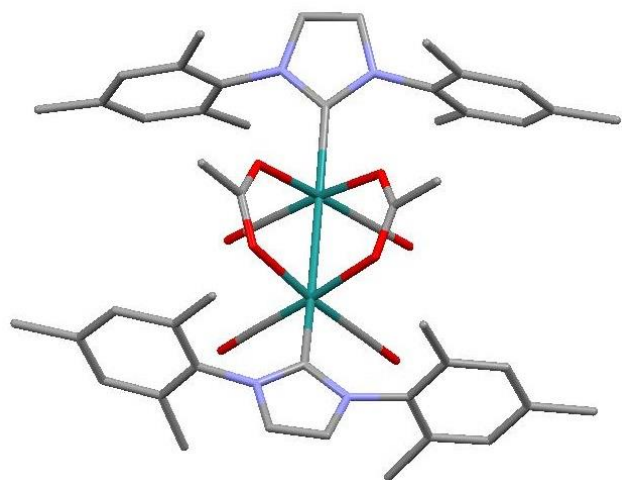
Received Date: 7 September 2015

Revised Date: 4 November 2015

Accepted Date: 5 November 2015

Please cite this article as: T.N. Rorhabaugh Jr., J.C. Doverspike, S.J. Geib, E.D. Sawyer, M.R. Stibbard, T.J. Malosh, Diruthenium tetracarbonyl sawhorse complexes bearing N-heterocyclic carbene and phosphine ligands: Synthesis, structural characterization, and catalytic activity, *Journal of Organometallic Chemistry* (2015), doi: 10.1016/j.jorganchem.2015.11.006.

This is a PDF file of an unedited manuscript that has been accepted for publication. As a service to our customers we are providing this early version of the manuscript. The manuscript will undergo copyediting, typesetting, and review of the resulting proof before it is published in its final form. Please note that during the production process errors may be discovered which could affect the content, and all legal disclaimers that apply to the journal pertain.



ACCEPTED MANUSCRIPT

Diruthenium tetracarbonyl sawhorse complexes bearing N-heterocyclic carbene and phosphine ligands: Synthesis, structural characterization, and catalytic activity

Thomas N. Rorhabaugh Jr.^a, Joshua C. Doverspike^a, Steven J. Geib^b, Evan D. Sawyer^a, Mitchell R. Stibbard^a, Thomas J. Malosh^{a,*}

^a *Department of Chemistry, University of Pittsburgh Johnstown, Johnstown, PA 15904, USA*

^b *Department of Chemistry, University of Pittsburgh, Pittsburgh, PA 15260, USA*

* Corresponding author. *Email address:* malosh@pitt.edu

ABSTRACT

A number of dinuclear ruthenium(I) sawhorse complexes substituted with an N-heterocyclic carbene or various phosphine ligands have been prepared and characterized by FT-IR, NMR, and elemental analysis. Treatment of $[\text{Ru}_2(\mu\text{-O}_2\text{CCH}_3)_2(\text{CO})_4]_n$ with 2-electron donating ligands (L) yields the dimeric derivatives $\text{Ru}_2(\mu\text{-O}_2\text{CCH}_3)_2(\text{CO})_4\text{L}_2$, where L = IMes [1,3-bis(2,4,6-trimethylphenyl)imidazol-2-ylidene] (**1**), $\text{P}(o\text{-CH}_3\text{C}_6\text{H}_4)_3$ (**2**), $\text{P}(\text{C}_6\text{F}_5)_3$ (**3**), $\text{P}(c\text{-C}_6\text{H}_{11})_3$ (**4**), and $\text{P}(\text{C}_6\text{H}_5)_3$ (**5**). The syntheses of **1-3** are reported herein; the syntheses of **4** and **5** have been previously reported. The crystal structures of **1-3** have been determined by single crystal X-ray diffraction. Factors influencing the structures of **1-5** are discussed and compared to DFT calculated geometries. An initial assay of the catalytic activities of **1-5**, employing the isomerization of 1-hexene, has been performed.

Keywords: Ruthenium; Dinuclear complexes; Catalysis; Carbene ligands; Phosphine ligands; Carboxylato bridges

Introduction

Interest in diruthenium(I) tetracarbonyl sawhorse-type compounds, $\text{Ru}_2(\mu\text{-O}_2\text{CCH}_3)_2(\text{CO})_4\text{L}_2$, particularly where L is a tertiary phosphine such as PBU_3 or PPh_3 , is due to their identification as catalysts or catalyst precursors for a variety of organic transformations. These transformations include the conversion of dimethyl oxalate to methyl glycolate and ethylene glycol [1], the conversion of acetic acid to ethyl acetate and methanol [2], the benzylation of phenol [3], alkene isomerization [4], the hydrogenation of alkenes and ketones [5], the semi-hydrogenation of diaryl alkynes [6], the hydrogenation of alkenes under scCO_2 conditions [7], and the hydroformylation of alkenes [8].

The sawhorse platform consists two pairs of eclipsed *cis*(carbonyl) legs, along with one pair of *cis*(bridging carboxylate) ligands as the trestle top - Scheme 1. This platform is quite robust and offers at least two opportunities for complex modification: alteration of the terminal or axial, two-electron donating ligands, L; and alteration of the three-electron donating *cis*(bridging) ligands. Indeed, while a variety of terminal ligands have been employed, a significant number of bridging ligands/systems, beyond carboxylates, have also been explored [9]. Regarding these bridging ligands, some recent work, involving carboxyphenyl porphyrin derivatives, has focused on the areas of molecular recognition [10], and photosensitizing/chemotherapeutic agents [7,11].

Spurred by successes in the area of palladium-based, catalytic carbon-carbon coupling [12], and ruthenium-based, catalytic ring closing olefin metathesis [13], the utilization of stable, N-heterocyclic carbenes as ligands in metal based catalytic systems has rapidly proliferated over the last twenty years. In addition to the above areas, it has been demonstrated that gold-NHC complexes can function as catalyst precursors for a variety of organic transformations [14]. In all three areas, it appears that N-heterocyclic carbenes have supplanted tertiary phosphines as the supporting ligands of choice [15].

In terms of the terminal ligand, L, we are interested in bringing both N-heterocyclic carbene ligands and heretofore unexamined tertiary phosphine ligands to bear upon the small molecule transformations mentioned above. Herein, we describe the synthesis and characterization of $\text{Ru}_2(\mu\text{-O}_2\text{CCH}_3)_2(\text{CO})_4\text{L}_2$, where L = IMes (**1**), $\text{P}(o\text{-tolyl})_3$ (**2**), and $\text{P}(\text{C}_6\text{F}_5)_3$ (**3**), including the solid-state structures of **1-3**. The synthetic protocol employed for **1-3** was extended to (**4**), L = PCy_3 . A procedure for the preparation of (**5**), L = PPh_3 , which has not been previously reported in detail is contained within. Also included are the results of DFT determined, geometric optimizations of **1-6**, where axial L = CO for (**6**). The isomerization of 1-hexene under mild conditions was utilized to assess the catalytic activities of **1-5**. In a study of alkene isomerization by select ruthenium compounds, η^2 -1-hexene intermediates have been proposed [16]. Optimized models of η^2 -1-hexene substituted complexes **1a-5a**, analogous to **1-5**, were calculated and the results are reported herein.

Results and discussion

Preparation and properties

In following the general procedure of Crooks *et al.* [17], we found that suspensions of the oligomeric starting material, $[\text{Ru}_2(\mu\text{-O}_2\text{CCH}_3)_2(\text{CO})_4]_n$, were slow to react with solutions of sterically bulky ligands such as PCy_3 . Adopting the approach of Hilts *et al.* [18], a *circa* 60 °C acetonitrile suspension of the oligomer provides the labile *bis*(acetonitrile) adduct as an intermediate. Both THF and the ultimate terminal ligand, L, were then added to the reaction vessel to provide the complexes $\text{Ru}_2(\mu\text{-O}_2\text{CCH}_3)_2(\text{CO})_4\text{L}_2$: L = 1,3-*bis*(2,4,6-trimethylphenyl)imidazol-2-ylidene: IMes (**1**), L = $\text{P}(o\text{-tolyl})_3$ (**2**), L = $\text{P}(\text{C}_6\text{F}_5)_3$ (**3**), and L = PCy_3 (**4**) - Scheme 1. The solid, yellow reaction residues were re-dissolved in either chloroform or dichloromethane, and recrystallization by slow diffusions of either ethanol or hexane,

provided compounds **1-4** in good yields. To our knowledge, complex **1** is the first reported diruthenium(I) sawhorse-type complex with terminal N-heterocyclic carbene ligands. A dry mixture of the oligomeric starting material and solid triphenylphosphine were heated beyond the melting point of PPh₃. After heating for 2 hours, the resulting yellow solution indicating the formation of Ru₂(μ-O₂CCH₃)₂(CO)₄(PPh₃)₂, (**5**). A series of diethyl ether triturations, followed by a diffusion of a saturated dichloromethane solution into hexane provided compound **5** in good yield.

Elemental Analysis (C, H) established purity for compounds **1-5**. In general, complexes **1-4** are soluble in chloroform and dichloromethane. Compound **1** is insoluble in pentane and hexane; soluble in toluene and THF; slightly soluble in diethyl ether; and insoluble in ethanol. Compound **2** is insoluble in pentane and hexane; soluble in toluene and THF; slightly soluble in diethyl ether; and insoluble in ethanol. Compound **3** is insoluble in pentane and hexane; slightly soluble in toluene and diethyl ether; soluble in THF; and insoluble in ethanol. Compound **4** reluctantly dissolves in chloroform and dichloromethane.

Solid-state structures

The molecular structures of **1-3** are presented in Figures 1-3. Relevant crystallographic and structural data can be found in Tables 1 and 2. Each ruthenium atom is located at the center of an irregular octahedron formed by coordination to five ligands, and with the sixth coordination site occupied by a ruthenium-ruthenium bond. The 2-electron donating axial carbene, or phosphine, ligands are located *trans* to the Ru-Ru bond, with each ruthenium-axial ligand bond being roughly, but not exactly, collinear to the Ru-Ru bond. The equatorial plane around each ruthenium center consists of a pair of μ-acetate ligands along with a pair of carbon monoxide

ligands, where both pairs of ligands are mutually *cis*. Thus, idealized structure presented in Scheme 1 is generally achieved by **1-3** in the solid-state, Figures 1-3.

A limited number of diruthenium sawhorse compounds featuring *bis*(acetate) bridges have been structurally characterized. When considering only those structures incorporating phosphine ligands [5,6,19a-e], previously reported ruthenium-ruthenium bond lengths range from 2.718(5) Å to 2.7614(10) Å. With Ru-Ru bond lengths of 2.6896(3) Å and 2.6918(2), respectively, **2** and **3** become the shortest examples to date, Table 2. When considering all *bis*(acetate) structures [5,6,19a-k], previously reported Ru-Ru bond lengths range from 2.672(1) Å to 2.7614(10) Å. With a bond length of 2.7805(3) Å, complex **1** possesses the longest Ru-Ru bond among *bis*(acetate) bridged sawhorse compounds, Table 2.

The steric requirements of N-heterocyclic-carbene ligands are unlike those attributed to the phosphine cone angle, Figure 1 [20]. In the solid-state structure of **1**, a plane constructed by using the four *o*-methyls of the *bis*(mesityl) substituents is approximately co-planar with the equatorial planes of the ruthenium octahedra. Furthermore, the planar mesityl substituents are substantially twisted with respect to the plane of the central imidazole ring, as interplane torsions approach 90°. Following the method advanced by Müller and Mingos [21], the phosphine cone-angles, as manifest in the solid-state, have been calculated for **2-5**, and are presented in Table 2. The calculated cone angles are comparable for **4** (164°) and **5** (154°), the PCy₃ and PPh₃ adducts, respectively, as these data are within the ranges found by the initial study. Also, comparing **4** and **5** with the Tolman cone angles provides results similar to those exhibited by the average crystallographic cone angles in the original study, where the Tolman cone angles are 170° and 145° for PCy₃ and PPh₃, respectively [22]. Müller and Mingos' work did not extend to either P(*o*-tolyl)₃ or P(C₆F₅)₃. For **2**, the calculated crystallographic cone angle is 176°, while the

putative cone angle for $P(o\text{-tolyl})_3$ is listed as 194° [22]. However, as visible in Figure 2, one tolyl substituent has rotated such that its *o*-methyl faces away from the equatorial plane of the ruthenium octahedron. Effectively then, the calculated cone angle for complex **2**, of 176° , can be considered that of a $PPh(o\text{-tolyl})_2$ adduct.

The ideal sawhorse configuration implies a $(L\text{-Ru-Ru-L})^\circ$ torsion of 0° , along with eclipsed carbon monoxide "legs," and strictly planar carboxylate bridges. As can be seen from the various torsions presented in Table 2, the solid-state conformations generally deviate from the ideal. For example, when considering only those *bis*(acetate) structures incorporating tertiary phosphine ligands [5,6,19b-e], previously reported $(P\text{-Ru-Ru-P})^\circ$ torsions range from $2.5(7)^\circ$ to $57.0(11)^\circ$ for the P^iPr_3 and the PPh_2Py (dppy) adducts, respectively. There is no correlation between either of the phosphine cone angles and the torsions along the backbone of the molecules. The carboxylate bridges themselves also have unique steric requirements as suggested by the torsions of the hexacarbonyl adduct, **6**. As evinced by the various torsions, the core of complex **1** approaches an ideal sawhorse conformation. However, the N-heterocyclic carbene ligands are not eclipsed, but offset by *circa* 11° . Finally, the solid-state structures of **1-3**, and **5**, are stabilized by variety of aromatic interactions. Additional details may be found in the Supplemental Information.

Spectroscopic characterization

Compounds **1-5** are yellow, air stable, crystalline powders, which have been characterized by infrared, proton NMR, fluorine-19 NMR (**3** only), phosphorus-31 NMR (**2-5** only), and elemental analysis. The infrared spectra of **1-5** exhibit the expected pattern of three (very strong-medium-very strong) bands attributed to carbonyl stretching, and zero to three additional weak bands/shoulders in the $2200\text{-}1800\text{ cm}^{-1}$ region. These carbon monoxide stretching frequencies

show an expected trend in the σ -donating abilities of the terminal ligands, L. The observed trend: IMes > PCy₃ > PPh₃ ~ P(*o*-tolyl)₃ > P(C₆F₅)₃. Additionally, all infrared spectra feature at least two bands assigned to the symmetric and asymmetric stretching of the carboxylate bridges, found in the 1600-1400 cm⁻¹ region. The phosphorus-31 NMR spectra of **2-5** each consist of a single signal, and the proton NMR spectra of **1-5** contain but one singlet assigned to the methyl substituents of the bridging acetate ligands. Furthermore, the ¹H NMR spectra of **2** and **4** are indicative of restricted rotation about the Ru-P bonds at ambient temperatures [5]. The fluorine-19 NMR spectrum of **3** exhibits three signals corresponding to the *ortho*, *meta*, and *para* fluorine substituents, respectively. The assignment of each signal to a specific ring position is based on both integration, and previous reports [23].

The infrared and NMR data support a solution configuration for **1-5** in which the terminal ligands and both of the bridging acetate ligands are symmetrically equivalent. Such equivalencies are achieved by the C_{2v} sawhorse configuration of Ru₂(μ -O₂CCH₃)₂(CO)₄L₂ in which the pairs of eclipsed, *cis*-carbonyl groups are the legs of the sawhorse. Thus, the solution configuration of **1-5** is consistent with the solid-state configurations, as illustrated in Scheme 1, and Figures 1-3. The IR bands, in the 2200-1800 cm⁻¹ region exhibited by **1-5** are listed in Table 3, along with relevant phosphorus-31 NMR results.

Computational studies of 1-6

The exaggerated backbone torsion (P-Ru-Ru-P)^o of complex **2** in the solid-state, prompted the calculation of optimized molecular geometries for **1-6**. The literature led to the Perdew, Burke, and Ernzerhof functional, as well as the Becke Three Parameter functional. Selected results, listed in Table 4, were provided by employing the Perdew, Burke, and Ernzerhof functional, with the Stuttgart/Dresden ECP for ruthenium, and the 6-31G(d) basis for any additional elements,

within *Gaussian09* [24]. Through all six models, the computations provided zero imaginary frequencies. With the inferred absence of intermolecular forces, the geometric parameters of the gas phase molecules show considerable adjustment, particularly with regard to the various torsions exhibited in the solid-state. Of interest, the backbone torsions both increase and decrease across **1-6**, with no discernable correlation to other geometric parameters. The main torsion decreases for both **2** (82.9° to 54.9°) and **4** (20.2° to 18.7°), while this torsion increases for **1, 3, 5** (21.1° to 43.5°), and **6**; with the torsions of **2** and **5** exhibiting the extremes. Among the tertiary phosphine adducts, **2-5**, every calculated phosphine cone angle increases. With the exception of **2**, there is a general increase in the (O-Ru-Ru-O)° and (C-Ru-Ru-C)° torsions. Regarding all three torsions, the various forces present in the solid-state appear to have the least effect on complexes **4** and **6**.

The solid-state structure of **2** exhibits two intramolecular close contacts between methyl group hydrogen atoms on the P(*o*-tolyl)₃ ligands and the oxygen atoms of the acetate bridges. Specifically: (1) C-H...O = 3.13 Å with H...O = 2.26 Å, and θ C-H-O = 150°; (2) C-H...O = 3.35 Å with H...O = 2.45 Å, and θ C-H-O = 156°. For crystallographic refinement, a riding model was employed for all hydrogen atoms. However, these two contacts persist in the calculated structure of **2**. Specifically (PBE0): (1) C-H...O = 3.17 Å with H...O = 2.16 Å, and θ C-H-O = 154°; (2) C-H...O = 3.66 Å with H...O = 2.60 Å, and θ C-H-O = 163°. Similarly, the solid-state structure of **4** exhibits two intramolecular close contacts between hydrogen atoms on the PCy₃ ligands and the oxygen atoms of the acetate bridges. Specifically: (1) C-H...O = 3.25 Å with H...O = 2.42 Å, and θ C-H-O = 142°; (2) C-H...O = 3.33 Å with H...O = 2.52 Å, and θ C-H-O = 138°. For crystallographic refinement, a riding model was also employed for all hydrogen atoms. Again however, the two contacts persist in the calculated structure of **4**.

Specifically (PBE0): (1) C-H...O = 3.23 Å with H...O = 2.32 Å, and θ C-H-O = 139°; (2) C-H...O = 3.27 Å with H...O = 2.38 Å, and θ C-H-O = 137°. The C-H-O angles of **4** are more acute than those of **2**. Recently, an updated definition of the hydrogen bond was endorsed. The catenated articles extend to observed characteristics and valid experimental criteria [25]. One criterion is that hydrogen bonding leads to characteristic proton magnetic resonance signatures. Specifically and typically, pronounced deshielding for H in X-H...Y-Z should be exhibited. In the ¹H NMR spectra of **2** and **4**, pronounced deshielding of the relevant protons was not observed.

Catalytic Assay of 1-5

Under a nitrogen atmosphere, 0.036 mmol of the appropriate sawhorse dimer (**1-5**) was dissolved in 10.0 mL of toluene. To these yellow solutions, 0.011 mol, of 1-hexene was added by syringe. The vessel was then placed in a 55 °C oil bath, with stirring, for 45 hours. Within moments, the various solutions changed color. Green solutions were observed for every trial, and the color persisted until the flasks were removed from the bath. The resulting mixtures were found to contain 1-hexene, plus 2- and 3-hexenes. The following activities were observed: P(C₆F₅)₃ > PCy₃ > PPh₃ > P(*o*-tolyl)₃ > IMes, Table 5. It is apparent that the P(C₆F₅)₃ adduct (**3**) is an efficient catalyst precursor under the stated conditions. There is no correlation between the observed catalytic activity and either the calculated or putative cone angles, Tables 2 and 5.

In a pressure vessel under more robust conditions [P(N₂) = 1 atm, T = 100 °C, t = 15 hrs], Matteoli, *et al.* exposed 1-hexene to three (3) tertiary phosphine adducts of *bis*(acetate) bridged ruthenium sawhorse complexes [5]. Isomerization was selected as this catalytic transformation involves but a single substrate. A correlation was observed between isomerization activity and the solid-state (P-Ru-Ru-P)^o torsion: P^tBu₃ > P^uBu₃ > PⁱPr₃; respective conversions = 42.4 % >

34.2 % > 7.4 %; respective torsions = 21.9° > 8.1° > 2.5°. Their rationale being that greater torsions along the backbone of the molecule provide progressively less hindered access to the ruthenium centers. Regarding the isomerization activities of **1-5**, the correlation, as observed by Matteoli, *et al.*, between percent conversion and backbone torsion does not hold, Tables 2 and 5. Among the tertiary phosphine adducts only, **2-5**, there are two inverse correlations between catalytic activity and solid-state, geometric parameters: (1) isomerization activity increases with decreasing (P-Ru-Ru-P)^o torsions, and (2) isomerization activity increases with decreasing Ru-P bond length, Tables 2 and 5. However, for **2-5**, the two inverse correlations between catalytic activity and geometric parameters do not hold for the DFT calculated molecular geometries, Tables 4 and 5.

Alkene isomerization, specifically that of 1-hexene, by phosphine substituted ruthenium carbonyl carboxylates was further examined by Salvini, *et al.* [16]. The diruthenium tetracarbonyl sawhorse complex $\text{Ru}_2(\mu\text{-O}_2\text{CCH}_3)_2(\text{CO})_4(\text{P}^n\text{Bu}_3)_2$ was studied in this context. Based on gas chromatography, infrared, and ³¹P NMR analyses, the authors postulate a mechanism involving the substitution of 1-hexene for one terminal phosphine ligand to initially form an η^2 -1-hexene intermediate. Starting with the minimum energy structures (PBE0/MWB28) for **1-5**, optimized geometries for complexes **1a-5a** were calculated, where one terminal carbene ligand, or one terminal phosphine ligand, was substituted by η^2 -1-hexene. Selected results are presented in Table 6. As illustrated in Figure 4, a characteristic of **1a-5a** is that the C1-C2 bond axis of the coordinated 1-hexene is roughly co-linear with an AcO-Ru-CO axis. Of the various parameters listed in Tables 4 and 6, the main torsions of **1a-5a** exhibit the largest changes from the calculated main torsions for **1-5**. Regarding the coordination of 1-hexene to the ruthenium centers, the average distance, **1a-5a**, from the ruthenium center to the

centroid of the C1-C2 bond of the 1-hexene is 2.283 Å, Table 6. However, the Ru-centroid distances of complexes **3a** and **4a** are 2.300 Å or greater, with an average of 2.303 Å. Complexes **3** and **4** also exhibit the highest isomerization activities, Table 5. The Ru-centroid distances of the remaining three putative intermediates (**1a**, **2a**, and **5a**) are all less than 2.300 Å, with an average of 2.269 Å. Using the Student's *t*-test, a comparison of these two mean distances reveals that, with 95% confidence, 2.303 Å is statistically different from 2.269 Å. A similar set of means can be constructed from the (L-Ru-Ru-centroid)^o main torsions, Table 6. Where again, the average torsion of **3a** and **4a** is statistically different from the average torsion of the remaining three modeled intermediates. However, the respective main torsions of **3a** (5.9°) and **4a** (23.8°) are also distinctly different from each other.

Experimental

General Information

All preparations were performed under dry gaseous nitrogen atmospheres using dual gas/vacuum manifolds and standard schlenk techniques and glassware. Recrystallizations of compounds **1-5** were performed under aerobic conditions. The various phosphine ligands were used as received from either Sigma-Aldrich or Strem. The compound 1,3-*bis*(2,4,6-trimethylphenyl)imidazol-2-ylidene (IMes) was obtained from Strem and was recrystallized from hexane prior to use. The various carbene and phosphine ligands were manipulated in glove bags under dry nitrogen atmospheres. Organic solvents meeting ACS specifications, or better, were employed and were degassed and saturated with dry nitrogen prior to use.

Synthesis of the starting material, acetatodicarbonylruthenium polymer, [Ru(O₂CCH₃)(CO)₂]_n, was accomplished by following a previously published procedure [17]. The compound Ru₃(CO)₁₂ was obtained from Sigma-Aldrich and was used as received. The

acetic acid was purified by the addition of acetic anhydride, followed by reflux over KMnO_4 and distillation under nitrogen.

Infrared spectra of starting materials and synthetic targets were recorded on a Perkin-Elmer Model 1600 FTIR instrument. A Bruker Spectrospin Ultrashield 300 MHz FT NMR instrument was employed to obtain ^1H and $^{31}\text{P}\{^1\text{H}\}$ spectra of both starting materials and synthetic targets, as well as ^1H spectra of the isomerization reaction mixtures. The ^{31}P chemical shifts are reported versus 85% H_3PO_4 . Single crystal X-ray structural analyses were performed at the Chemistry Department X-ray Diffraction Facility at the University of Pittsburgh, Pittsburgh, PA, USA. At the Indiana University of Pennsylvania, Indiana, PA, USA, an Agilent 6890N Gas Chromatograph with a 5973 Mass Selective Detector was employed to obtain chromatographs of the isomerization reaction mixtures. Fluorine-19 NMR was performed at Spectral Data Services, Inc., located in Champaign, IL, USA. The ^{19}F chemical shifts are reported versus C_6F_6 . Elemental Analyses were performed at Atlantic Microlab, Inc., located in Norcross, GA, USA.

Preparation of dimeric complexes 1-4: $\text{Ru}_2(\mu\text{-O}_2\text{CCH}_3)_2(\text{CO})_4\text{L}_2$

The dimeric, symmetric *bis*(substituted) complexes, **1-4**, were prepared by the addition of a carbene or phosphine ligand to the *bis*(acetonitrile) adduct, $\text{Ru}_2(\mu\text{-O}_2\text{CCH}_3)_2(\text{CO})_4(\text{CH}_3\text{CN})_2$, in the manner advanced by Hilts *et al.* [18].

Typical preparation: 3 mL of sparged acetonitrile were added by syringe to a 3-neck, 100-mL RBF, with gas inlet, containing 200 mg (0.463 mmol) of $[\text{Ru}_2(\mu\text{-O}_2\text{CCH}_3)_2(\text{CO})_4]_n$. With stirring under N_2 , the flask was placed in a 60 °C oil bath for 2 hours. The resulting yellow solution indicates full dissolution of the intractable, orange starting material, and the formation of $\text{Ru}_2(\mu\text{-O}_2\text{CCH}_3)_2(\text{CO})_4(\text{CH}_3\text{CN})_2$. After removal from the oil bath, a 20.0 mL aliquot of THF was transferred to the flask. A solid addition funnel was then used to add a slight excess of ligand

(circa 1.0 mmol). The mixture was returned to the oil bath, with stirring under N₂, for an additional 2 hours. The solvents were then removed under reduced pressure to yield a mixture of Ru₂(μ-O₂CCH₃)₂(CO)₄L₂ plus excess ligand, L.

Ru₂(μ-O₂CCH₃)₂(CO)₄(C₂₁H₂₄N₂)₂: bis(IMes) adduct (1)

The reaction residue was dissolved in minimal dichloromethane. Under ambient conditions, a layer of hexane was allowed to slowly diffuse into the dichloromethane solution of the complex. The resulting pale yellow crystals were collected on a sintered glass crucible, washed with chilled hexane, and dried under vacuum. Yield: (379 mg, 0.364 mmol, 79%). IR (CHCl₃, cm⁻¹) ν(CO): 2005 (vs), 1951 (m), 1922 (vs), 1887 (w); ν(CO₂): 1579 (m), 1438 (m). ¹H NMR (300 MHz, CDCl₃) δ: 6.87 (m, 12H), 2.31 (s, 12H), 2.10 (s, 24H), 1.19 (s, 6H, OAc). Anal. Calc. for C₅₀H₅₄N₄O₈Ru₂: C, 57.68; H, 5.23; N, 5.38. Found: C, 57.84; H, 5.34; N, 5.40%.

*Ru₂(μ-O₂CCH₃)₂(CO)₄{P(*o*-CH₃C₆H₄)₃}₂: bis(tri-*o*-tolylphosphine) adduct (2)*

The reaction residue was dissolved in minimal chloroform. Under ambient conditions, a layer of hexane was allowed to slowly diffuse into the chloroform solution of the complex. The resulting yellow crystals were collected on a sintered glass crucible, washed with chilled hexane, and dried under vacuum. Yield: (415 mg, 0.399 mmol, 86%). IR (CHCl₃, cm⁻¹) ν(CO): 2025 (vs), 1982 (m), 1951 (vs), 1920 (w); ν(CO₂): 1573 (m), 1440 (m). ¹H NMR (300 MHz, CD₂Cl₂) δ: 7.28 (m, 24H), 2.17 (s, br 24H). ³¹P{¹H} NMR (121 MHz, CDCl₃) δ: 14.67 (s). Anal. Calc. for C₅₀H₄₈O₈P₂Ru₂: C, 57.69; H, 4.65. Found: C, 57.64; H, 4.75%.

Ru₂(μ-O₂CCH₃)₂(CO)₄{P(C₆F₅)₃}₂: bis(tris(pentafluorophenyl)phosphine) adduct (3)

The reaction residue was dissolved in minimal chloroform. Under ambient conditions, a layer of ethanol was allowed to slowly diffuse into the chloroform solution of the complex. The resulting yellow crystals were collected on a sintered glass crucible, washed with chilled ethanol, and

dried under vacuum. Yield, based on chloroform solvate: (482 mg, 0.298 mmol, 64%). IR (CHCl₃, cm⁻¹) $\nu(\text{CO})$: 2047 (vs), 2008 (m), 1979 (vs), 1953 (w); $\nu(\text{CO}_2)$: 1572 (m), 1448 (m). ¹H NMR (300 MHz, CDCl₃) δ : 1.45 (s, 6H, OAc). ¹⁹F NMR (376 MHz, CDCl₃) δ : -127.31 (s, 12F, o), -147.32 (s, 6F, p), -160.31 (t, 12F, m). ³¹P{¹H} NMR (121 MHz, CDCl₃) δ : -28.85 (m). Anal. Calc. for C₄₄H₆F₃₀O₈P₂Ru₂·CHCl₃: C, 33.45; H, 0.44. Found: C, 33.73; H, 0.32%.

*Ru₂(μ -O₂CCH₃)₂(CO)₄{P(*c*-C₆H₁₁)₃}₂: bis(tricyclohexylphosphine) adduct (4)*

The reaction residue was dissolved in minimal chloroform. Under ambient conditions, a layer of ethanol was allowed to slowly diffuse into the chloroform solution of the complex. The resulting yellow crystals were collected on a sintered glass crucible, washed with chilled ethanol, and dried under vacuum. Yield: (261 mg, 0.263 mmol, 57%). IR (CHCl₃, cm⁻¹) $\nu(\text{CO})$: 2010 (vs), 1962 (m), 1933 (vs), 1900 (w); $\nu(\text{CO}_2)$: 1579 (m), 1436 (m). ¹H NMR (300 MHz, C₆D₆) δ : 2.21 (s, br 6H, OAc), 1.97-1.29 (all m, br 66H). ³¹P{¹H} NMR (121 MHz, CDCl₃) δ : 25.17 (s). Anal. Calc. for C₄₄H₇₂O₈P₂Ru₂: C, 53.21; H, 7.31. Found: C, 53.57; H, 7.46%.

Preparation of the dimeric complex 5: Ru₂(μ -O₂CCH₃)₂(CO)₄(PPh₃)₂, via fusion

Ru₂(μ -O₂CCH₃)₂(CO)₄{P(C₆H₅)₃}₂: bis(triphenylphosphine) adduct (5)

A 50-mL RBF, with a gas inlet, was charged with 200 mg (0.462 mmol) of [Ru₂(μ -O₂CCH₃)₂(CO)₄]_n and 1.5 g of triphenylphosphine (*circa* 5 equivalents). With stirring under N₂, the flask was placed in a 90 °C oil bath for 2 hours. After cooling, the pale yellow solid was triturated with diethyl ether - 3x. The resulting yellow residue was dissolved in minimal dichloromethane. Under ambient conditions, a layer of hexane was allowed to slowly diffuse into the dichloromethane solution of the complex. The resulting yellow-orange crystals were collected on a sintered glass crucible, washed with chilled hexane, and dried under vacuum. Yield: (390 mg, 0.408 mmol, 88%). IR (CHCl₃, cm⁻¹) $\nu(\text{CO})$: 2023 (vs), 1978 (m), 1949 (vs),

1919 (w); $\nu(\text{CO}_2)$: 1569 (m), 1436 (m). ^1H NMR (300 MHz, CDCl_3) δ : 7.55 (m, 12H), 7.40 (m, 18H), 1.69 (s, 6H, OAc). $^{31}\text{P}\{^1\text{H}\}$ NMR (121 MHz, CDCl_3) δ : 14.39 (s). Anal. Calc. for $\text{C}_{44}\text{H}_{36}\text{O}_8\text{P}_2\text{Ru}_2$: C, 55.23; H, 3.79. Found: C, 55.13; H, 3.87%.

Crystallographic analyses

Diffraction quality, off-white crystals of compound **1** were formed as hexane diffused into a saturated dichloromethane solution under ambient conditions. Diffraction quality, yellow crystals of compounds **2** and **4** were obtained as ethanol diffused into saturated chloroform solutions under ambient conditions. Diffraction quality, yellow crystals of compound **3** were formed as hexane diffused into a saturated chloroform solution under ambient conditions. The studied crystals were mounted on glass capillaries and data was collected on a Bruker SMART Apex II CCD system utilizing an I μ S micro-focus source to provide Cu K α radiation at $\lambda = 1.54178$ Å. Detailed crystallographic data for **1-3** are listed in Table 1. Other relevant, structural information is presented in Table 2. A structure for $\text{Ru}_2(\text{CO})_4(\mu\text{-O}_2\text{CCH}_3)_2(\text{PCy}_3)_2$ has been previously deposited in the Cambridge Structural Database [6]. Additional detail regarding the crystallographic analysis of **4** can be found in the Supplemental Information.

Compounds **1** and **3**. Systematic absences were consistent with the space groups $\text{P}2_1/c$ and $\text{C}2/c$, for **1** and **3**, respectively. For both compounds, data were corrected for absorption effects using multi-scan methods (SADABS), absorption coefficients: $\mu = 5.522 \text{ mm}^{-1}$ and 6.527 mm^{-1} for **1** and **3** respectively. The resulting 6943 data and 4377 data, for **1** and **3** respectively, were employed in the least squares refinements. Compound **2**. The triclinic unit cell was consistent with either space group $\text{P}i$, or $\text{P}\bar{1}$. The average values of the normalized structure factors favored $\text{P}\bar{1}$. The data were corrected for absorption effects using the multi-scan method (SADABS),

absorption coefficient: $\mu = 7.185 \text{ mm}^{-1}$. The resulting 15785 data were used in the least squares refinements.

Compounds **1-3**. All three structures were solved by employing direct methods within the SHELXTL software package [26]. The correct positions for the ruthenium and phosphorous atoms were deduced from a direct methods E-map. Subsequent least squares refinement and difference Fourier calculations established the positions of the remaining non-hydrogen atoms. Non-hydrogen atoms were refined with independent anisotropic displacement parameters. Hydrogen atoms were fixed in idealized positions and their displacement parameters were tied to those of the attached non-hydrogen atom. All structures were refined by full matrix, least squares procedures, based on F^2 , of the positional, isotropic, and anisotropic thermal parameters for all non-hydrogen atoms. A final analysis of variance between calculated and observed structure factors exhibited no perceptible errors. PLATON was used to calculate a number of geometric parameters [27].

Computational studies

Hybrid density functional theory calculations were performed to ascertain optimal molecular geometries for complexes **1-6**. As the starting point for the geometric optimizations, solid-state structures were used to provide the molecular specifications for *Gaussian09* [24]. The X-ray structures of **1-3** are reported herein, and that of **4** in the Supplemental Information. Previously reported structural data was used for **5** [19b]. The deposited solid-state structure of $\text{Ru}_2(\text{CO})_4(\mu\text{-O}_2\text{CCH}_3)_2(\text{CO})_2$ (**6**) does not include any positional data for the six hydrogen atoms [19f]. A model of **6** was constructed and optimized using Scigress computational software [28]. This optimized model was employed as the molecular specification in lieu of complete CIF information.

Within *Gaussian09*, the Perdew, Burke, and Ernzerhof functional (PBE0) was employed. The basis set was composed of the Stuttgart/Dresden ECP for ruthenium (MWB28), along with the 6-31G(d) basis for any additional elements. Normal-mode analyses were then performed on the optimized geometries. Selected results are presented in Table 4. Additionally, geometric optimizations were obtained by utilizing the Becke Three Parameter functional with the LYP correlation functional (B3LYP). The basis was composed of the Los Alamos ECP plus DZ for ruthenium (LanL2DZ), along with the 6-31G(d) basis for any additional elements. Normal-mode analyses were then performed on the optimized geometries. Selected results are presented in Table 4S (Supplemental Information).

Optimized structures were also calculated for a series of complexes, **1a-5a**, where one terminal carbene or phosphine ligand was replaced by η^2 -1-hexene. As the starting point for the geometric optimizations, the minimum energy structures for **1-5**, above, were used to provide the molecular specifications for *Gaussian09*. An idealized molecule of 1-hexene was constructed and optimized using Scigress computational software [28]. The 1-hexene model was then substituted for the appropriate terminal ligand. Within *Gaussian09*, the Perdew, Burke, and Ernzerhof functional (PBE0) was employed. The basis set was composed of the Stuttgart/Dresden ECP for ruthenium (MWB28), along with the 6-31G(d) basis for any additional elements. Normal-mode analyses were then performed on the optimized geometries. Selected results are presented in Table 6.

Isomerization of 1-hexene in the presence of 1-5

Representative procedure: 10 mL of sparged toluene were added by syringe to a 50-mL RBF, with gas inlet and condenser, containing 0.036 mmol of diruthenium sawhorse compound.

Finally, 1.4 mL (0.011 mol) of 1-hexene were added by syringe. With stirring under N₂, the flask was placed in a 55 °C oil bath for 45 hours.

The reaction mixtures were examined by both proton NMR and gas chromatography (GCMS). The average results, by adduct, are listed in Table 5.

Conclusions

Compounds **1-3** are readily synthesized by the addition of two equivalents of the desired axial ligand to the labile intermediate Ru₂(μ-O₂CCH₃)₂(CO)₄(NCCH₃)₂ in THF. Compound **5** can be synthesized via a fusion obtained from suspending oligomeric [Ru₂(μ-O₂CCH₃)₂(CO)₄]_n in liquid triphenylphosphine. The solid-state structures of **1-3** exhibit the expected sawhorse conformation. However, the various torsions achieved by **1-6** in the solid-state show numerous departures from an ideal conformation. Spectroscopic characterization affirms a C_{2v} arrangement about the ruthenium centers. The Ru-Ru bond lengths of **1-3**, and the P-Ru-Ru-P torsion angles of **1** and **2** are structurally significant. The extent of the phosphine cone angles, as achieved by **2-5** in the solid-state, have been calculated. Comparatively, the calculated cone angles of **4** and **5** fall within the limits of the original study. The calculated cone angle of **5** exceeds the Tolman cone angle, whereas those of **2-4** fall short. Close X-H...Y-Z contacts are found in the solid-state structures of **2** and **4**, and these contacts persist in the respective DFT optimized geometries. However, spectroscopic evidence of intramolecular hydrogen bonding is lacking. Regarding the solid-state torsions displayed by **1-6**, the DFT results show numerous, irregular adjustments in the gas-phase conformations. Compounds **1-5** are catalytic precursors toward the isomerization of 1-hexene under mild conditions. The compounds display a broad range of capabilities. Among **1-5**, the isomerization activity of the P(C₆F₅)₃ adduct (**3**) is markedly different. DFT calculated models of the proposed η²-1-hexene intermediates,

constructed from the most active catalyst precursors, possess a longer average Ru-hexene(centroid) distance than those built from less active adducts.

Acknowledgements

We gratefully acknowledge the Mentorship Fund for Faculty/Student Scholarship at the University of Pittsburgh Johnstown for partial financial support of this project. T.J.M. thanks Dr. Justin D. Fair at IUP, Dr. Robert Grimminger, and David R. Swanger III for their valuable contributions.

Appendix A. Supplementary Data

CCDC 1418271, 1418272, 1418273, 1418274 contain the supplementary crystallographic data for this paper. These data can be obtained free of charge from the Cambridge Crystallographic Data Centre via www.ccdc.cam.ac.uk/data_request/cif.

References

- [1] (a) U. Matteoli, M. Bianchi, G. Menchi, P. Frediani, F. Piacenti, *J. Mol. Catal.* 29 (1985) 269;
(b) U. Matteoli, G. Menchi, M. Bianchi, F. Piacenti, *J. Organomet. Chem.* 299 (1986) 233;
(c) U. Matteoli, G. Menchi, M. Bianchi, F. Piacenti, *J. Mol. Catal.* 44 (1988) 347;
(d) U. Matteoli, G. Menchi, M. Bianchi, F. Piacenti, *J. Mol. Catal.* 64 (1991) 257.
- [2] (a) M. Bianchi, G. Menchi, F. Francalanci, F. Piacenti, U. Matteoli, P. Frediana, C. Botteghi, *J. Organomet. Chem.* 188 (1980) 109;
(b) U. Matteoli, G. Menchi, M. Bianchi, P. Frediani, F. Piacenti, *Gazz. Chim. Ital.* 115 (1985) 603;
(c) P. Frediani, M. Bianchi, A. Salvini, F. Piacenti, S. Ianelli, M. Nardelli, *J. Chem. Soc., Dalton Trans.* (1990) 1705;
(d) A. Salvini, P. Frediani, C. Gianelli, L. Rosi, *J. Organomet. Chem.* 690 (2005) 371.
- [3] R. Jaouhari, *Chem. Lett.* 23 (1994) 1781.
- [4] A. Salvini, P. Frediani, D. Rovai, M. Bianchi, F. Piacenti, *J. Mol. Catal.* 89 (1994) 77.
- [5] U. Matteoli, G. Menchi, M. Bianchi, F. Piacenti, S. Ianelli, M. Nardelli, *J. Organomet. Chem.* 498 (1995) 177.

- [6] J. Li, R. Hua, *Chem. Eur. J.* 17 (2011) 8462.
- [7] J.P. Johnpeter, L. Plasseraud, F. Schmitt, L. Juillerat-Jeanneret, B. Therrien, *J. Coord. Chem.* 66 (2013) 1753.
- [8] (a) J. Jenck, P. Kalck, E. Pinelli, M. Siani, A. Thorez, *J. Chem. Soc., Chem. Commun.* (1988) 1428;
(b) P. Kalck, M. Siani, J. Jenck, B. Peyrille, Y. Peres, *J. Mol. Catal.* 67 (1991) 19.
- [9] B. Therrien, G. Suss-Fink, *Coord. Chem. Rev.* 253 (2009) 2639.
- [10] J.P. Johnpeter, J. Mohanraj, N. Amaroili, B. Therrien, *Eur. J. Inorg. Chem.* (2012) 3449.
- [11] (a) J.P. Johnpeter, F. Schmitt, E. Denoyelle-Di-Muro, G. Wagnieres, L. Juillerat-Jeanneret, B. Therrien, *Inorg. Chim. Acta* 393 (2012) 246.
(b) J.P. Johnpeter, B. Therrien, *Inorg. Chim. Acta* 394 (2013) 723.
- [12] W.A. Herrmann, M. Elison, J. Fischer, C. Kocher, G.R.J. Artus, *Angew. Chem. Int. Ed. Engl.* 34 (1995) 2371.
- [13] M. Scholl, T.M. Trnka, J.P. Morgan, R.H. Grubbs, *Tetrahedron Lett.* 40 (1999) 2247.
- [14] S.P. Nolan, *Acc. Chem. Res.* 44 (2011) 91.
- [15] D.J. Nelson, *Eur. J. Inorg. Chem.* (2015) 2012.
- [16] A. Salvini, P. Frediani, F. Piacenti, *J. Mol. Catal. A* 159 (2000) 185.
- [17] G.R. Crooks, B.F.G. Johnson, J. Lewis, I.G. Williams, G. Gamlen, *J. Chem. Soc. A* (1969) 2761.
- [18] R.W. Hiltz, M. Cowie, *Inorg. Chem.* 29 (1990) 3349.
- [19] (a) T.A. Bright, R.A. Jones, C.M. Nunn, *J. Coord. Chem.* 18 (1988) 361.
(b) K-B. Shiu, S-M. Peng, M-C. Cheng, *J. Organomet. Chem.* 452 (1993) 143.
(c) J.S. Field, R.J. Hines, C.J. Parry, *J. Chem. Soc., Dalton Trans.* (1997) 2843.
(d) T.J. Malosh, S.R. Wilson, J.R. Shapley, *J. Organomet. Chem.* 694 (2009) 3331.
(e) P. Stepnicka, I. Cisarova, *Collect. Czech. Chem. Commun.* 74 (2009) 799.
(f) M. Spohn, T. Vogt, J. Straehle, *Z. Naturforsch., B: Chem. Sci.* 41 (1986) 1373.

- (g) R.W. Hiltz, S.J. Sherlock, M. Cowie, E. Singleton, M.M. de V. Steyn, *Inorg. Chem.* 29 (1990) 3161.
- (h) K. Panneerselvam, T-H. Lu, C-H. Huang, S-F. Tung, K-B. Shiu, *Acta Crystallogr., Sect. C: Cryst. Struct. Commun.* 53 (1997) 1782.
- (i) C.M. Kepert, G.B. Deacon, L. Spiccia, G.D. Fallon, B.W. Skelton, A.H. White, *J. Chem. Soc., Dalton Trans.* (2000) 2867.
- (j) C.M. Kepert, G.B. Deacon, L. Spiccia, *Inorg. Chim. Acta* 355 (2003) 213.
- (k) R. Dorta, G. Suss-Fink, H. Stoeckli-Evans, *Acta Crystallogr., Sect. E: Struct. Rep. Online* 60 (2004) m1397.
- [20] A.C. Miller, W.J. Sommer, B.S. Yong, J.L. Petersen, L. Cavallo, S.P. Nolan, *Organometallics* 22 (2003) 4322.
- [21] T.E. Müller, D.M.P. Mingos, *Transition Met. Chem.* 20 (1995) 533.
- [22] C.A. Tolman, *Chem. Rev.* 77 (1977) 313.
- [23] (a) M.G. Barlow, M. Green, R.N. Haszeldine, H.G. Higson, *J. Chem. Soc. B* (1966) 1026.
(b) M.G. Hogben, W.A.G. Graham, *J. Am. Chem. Soc.* 91 (1969) 283.
- [24] M.J. Frisch, *et al.*, *Gaussian09*, Revision D.01 WIN64 (2009) Gaussian, Inc.: Wallingford, CT.
- [25] (a) E. Arunan, G.R. Desiraju, R.A. Klein, J. Sadlej, S. Scheiner, I. Alkorta, D.C. Clary, R.H. Crabtree, J.J. Dannenberg, P. Hobza, H.G. Kjaergaard, A.C. Legon, B. Mennucci, D.J. Nesbitt, *Pure Appl. Chem.* 83 (2011) 1619.
(b) E. Arunan, G.R. Desiraju, R.A. Klein, J. Sadlej, S. Scheiner, I. Alkorta, D.C. Clary, R.H. Crabtree, J.J. Dannenberg, P. Hobza, H.G. Kjaergaard, A.C. Legon, B. Mennucci, D.J. Nesbitt, *Pure Appl. Chem.* 83 (2011) 1637.
- [26] G.M. Sheldrick, *SHELXTL*, version 6.10 (2001) Bruker Analytical X-ray Systems: Madison, WI.
- [27] A.L. Spek, *PLATON: A Multipurpose Crystallographic Tool*, Utrecht University, 2005.
- [28] *DGauss4.1*, Oxford Molecular, Fujitsu Ltd., 2000.

Table 1
Crystal data and refinement parameters for 1-3.

Adduct:	IMes (1)	P(<i>o</i> -tolyl) ₃ (2)	P(C ₆ F ₅) ₃ (3)
formula	C ₅₀ H ₅₄ N ₄ O ₈ Ru ₂	C ₅₀ H ₄₈ O ₈ P ₂ Ru ₂	C ₄₄ H ₆ F ₃₀ O ₈ P ₂ Ru ₂
formula wt.	1041.11	1040.96	1496.57
crystal system	monoclinic	monoclinic	triclinic
space group	P2 ₁ /c	C2/c	P-1
a, Å	13.8985(4)	10.5074(3)	9.9245(4)
b, Å	14.9593(4)	14.8416(8)	21.3845(8)
c, Å	23.3482(7)	29.3597(9)	23.7181(9)
α, deg	90	90	101.969(2)
β, deg	95.947(1)	99.364(1)	92.086(2)
γ, deg	90	90	94.221(2)
Volume, Å ³	4828.2(2)	4517.5(2)	4904.0(3)
Z	4	4	4
Temp, K	230(2)	293(2)	230(2)
ρ _{calcd} , g/cm ³	1.432	1.531	2.027
μ, mm ⁻¹	5.522	6.527	7.185
total data	8808	4413	17353
unique data	6943	4377	15785
parameters	607	284	1565
R _{int}	0.0547	0.1175	0.0272
R ₁ (all data) ^a	0.0498	0.0376	0.0283
wR ₂ (all data) ^b	0.1038	0.1034	0.0811
max, min, e/Å ³	1.591, -0.637	2.047, -1.459	0.477, -0.573

$$^a R_1 = \sum ||F_o| - |F_c|| / \sum |F_o|, \quad ^b wR_2 = [\sum w(F_o^2 - F_c^2)^2 / \sum w(F_o)^2]^{1/2}$$

Table 2Crystal Data: Selected bond lengths (Å), torsions (°), and angles (°) for **1-6**^a

Adduct:	IMes	P(<i>o</i> -tolyl) ₃	P(C ₆ F ₅) ₃	PCy ₃	PPh ₃	CO
Ru-Ru	2.7805(3)	2.6896(3)	2.6918(2)	2.7555(6)	2.7360(9)	2.6881(15)
Ru-L	2.184(3)	2.5235(4)	2.4370(6)	2.4496(12)	2.4508(10)	1.988(9)
P-C avg.		1.848(2)	1.840(1)	1.864(1)	1.824(1)	
L-Ru-Ru-L	0.9(5)	82.89(18)	19.11(14)	20.2(3)	21.14(11)	3.7(18)
O-Ru-Ru-O ^b	1.05(9)	18.29(6)	13.61(7)	5.07(11)	1.47(8)	9.8(3)
C-Ru-Ru-C ^c	1.21(14)	31.10(9)	17.00(13)	2.9(2)	2.67(14)	10.2(6)
Ru-P-C avg.		114.18(6)	115.64(6)	114.05(11)	115.1(3)	
Cone Angle ^d		176	167	164	154	
Cone Angle ^e		194	184	170	145	

a) **1-4**, this work; **5** [18b]; **6** [18f] *b*) avg. QAc bridges *c*) avg. CO ligands *d*) calculated avg., [21] *e*) Tolman, [22]

Table 3Selected spectral data for **1-5**.

Ru ₂ (μ-OAc) ₂ (CO) ₄ L ₂		IR ν(CO) ^a cm ⁻¹				NMR ³¹ P{ ¹ H} ^c		
Ligand	(vs)	(m)	(vs)	(w)	δ(ppm) ligand	δ(ppm) complex	ΔP(ppm) complex	
3 P(C ₆ F ₅) ₃	2047	2008	1979	1953	-74.26	-28.85	45.41	
2 P(<i>o</i> -tolyl) ₃	2025	1982	1951	1920	-29.64	14.67	44.31	
5 PPh ₃	2023	1978	1949	1919	-5.41	14.39	19.80	
4 PCy ₃	2010	1962	1933	1900	6.11	25.17	19.06	
1 IMes ^b	2005	1951	1922	1887				

a) CHCl₃, this work *b*) 1,3-bis(2,4,6-trimethylphenyl)imidazol-2-ylidene *c*) vs. H₃PO₄, this work

Table 4**Optimized Models: Geometric parameters in (Å) and (°) for 1-6^a**

Complex:	1	2	3	4	5	6
Ru-Ru	2.771	2.722	2.684	2.752	2.700	2.729
Ru-L	2.166	2.509	2.423	2.448	2.437	1.961
P-C		1.851	1.842	1.871	1.836	
L-Ru-Ru-L	13.3	54.9	29.9	18.7	43.5	5.0
O-Ru-Ru-O ^b	13.1	15.5	17.0	10.2	18.5	9.8
C-Ru-Ru-C ^c	17.5	22.1	24.1	9.1	24.9	11.0
Ru-P-C avg.		114.3	115.5	113.8	115.1	
Cone Angle ^d		179	169	167	158	
Cone Angle ^e		194	184	170	145	

a) PBE0/MWB28 *b)* avg. QAc, *c)* avg. CO, *d)* calc. avg., [21] *e)* Tolman, [22]

Table 5Isomerization of 1-hexene to 2- and 3-hexenes upon exposure to **1-5** in toluene^a

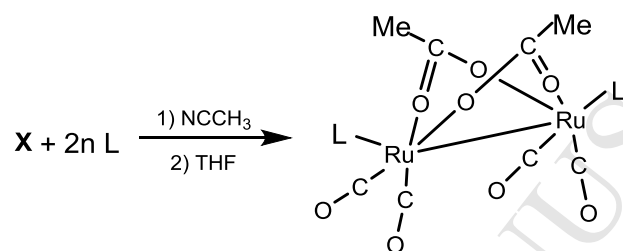
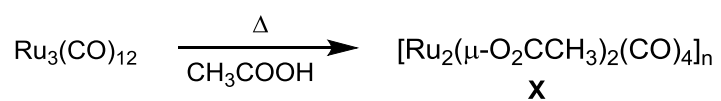
Adduct:	P(C ₆ F ₅) ₃ (3)	PCy ₃ (4)	PPh ₃ (5)	P(<i>o</i> -tolyl) ₃ (2)	IMes (1)
Conversion %:	67.4	20.2	15.1	12.1	1.0

^a) conditions: P(N₂) = 1 atm., T = 55 °C, t = 45 hrs., dimer = 0.036 mmol, substrate = 0.011 mol

Table 6**Optimized Intermediates: Parameters in (Å) and (°) for 1a-5a^a**

Complex:	1a	2a	3a	4a	5a
Ru-Ru	2.733	2.717	2.681	2.729	2.701
Ru-centroid ^b	2.287	2.270	2.300	2.306	2.251
Ru-L	2.147	2.503	2.427	2.449	2.432
P-C		1.851	1.843	1.871	1.835
L-Ru-Ru-cent.	45.8	56.0	5.9	23.8	60.7
O-Ru-Ru-O ^c	14.7	13.8	17.7	12.4	16.4
C-Ru-Ru-C ^d	20.9	18.6	23.7	14.0	22.8
Ru-P-C avg.		114.1	115.5	113.7	115.0
Cone Angle ^e		179	169	167	158
Cone Angle ^f		194	184	170	145

a) PBE0, b) C1-C2 centroid, c) avg. OAc, d) avg. CO, e) calc., [21] f) Tolman, [22]



Scheme 1

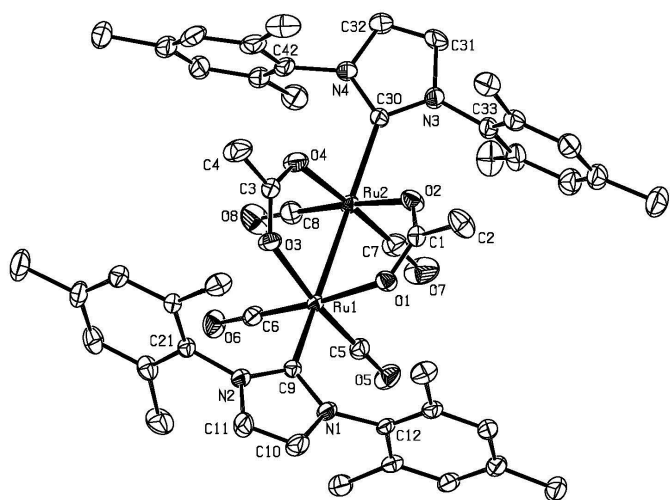


Fig. 1. ORTEP diagram (40%) of **1**, with hydrogen atoms omitted.

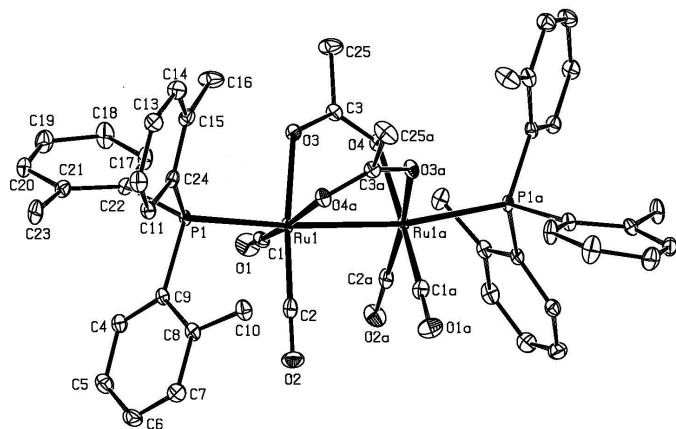


Fig. 2. ORTEP diagram (40%) of **2**, with hydrogen atoms omitted.

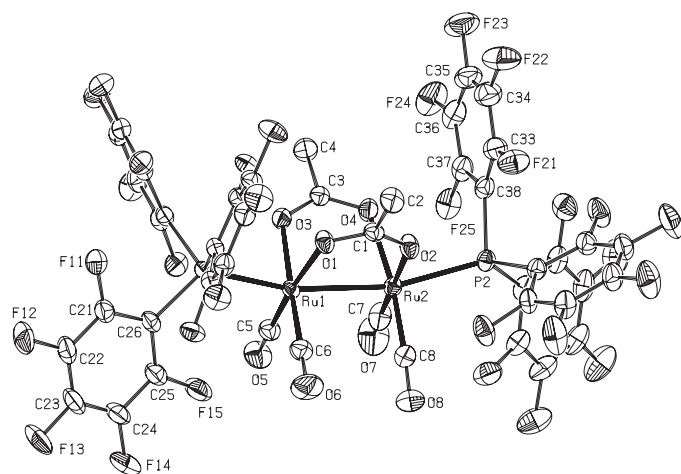


Fig. 3. ORTEP diagram (40%) of **3**, with hydrogen atoms omitted.

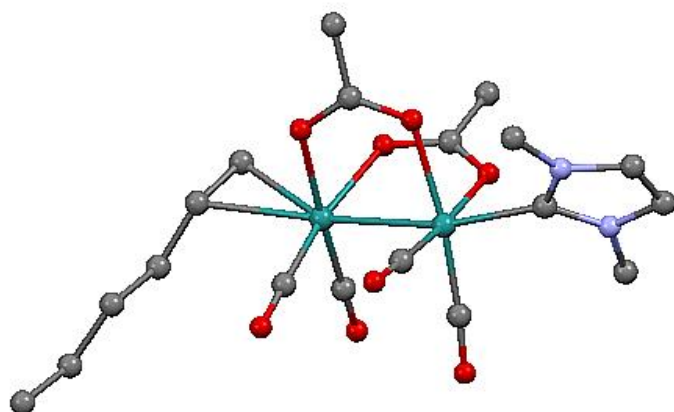


Fig. 4. Calculated structure of **1a**, an η^2 -1-hexene intermediate. Hydrogen atoms and carbene substituents omitted for clarity.

ACCEPTED MANUSCRIPT

- The first diruthenium tetracarbonyl sawhorse NHC adduct is reported.
- An assay of catalytic ability, mild conditions, reveals a distinctly active complex.
- DFT calculations were performed to support experimental results.
- Phosphine cone angles, as achieved in the solid-state, have been calculated.